Laser and Particle Beams (2005), *23*, 513–519. Printed in the USA.

DOI: 10.1017/S026303460505069X

Laser-produced blast wave and numerical simulation using the FLASH code

D.R. FARLEY,[1,2] K. SHIGEMORI,[1] AND H. AZECHI[1]
[1]Institute of Laser Engineering, Osaka University, Suita, Osaka Japan
[2]EPRI Worldwide, Palo Alto, California

(RECEIVED 30 March 2005; ACCEPTED 16 May 2005)

Abstract

Two-dimensional (2D) FLASH simulations were run with Spitzer-Härm conductivity on and off in an attempt to simulate a laser-produced blast wave. Dissociation, ionization, recombination, and radiative cooling were not included. An initial Gaussian temperature profile with $T_0 = 120$ eV and spot radius $r_0 = 25$ μm was used assuming 1 μm thickness of the CH disk is ablated into the background nitrogen gas. Evolution of the blast wave differs slightly between the cases of Spitzer-Härm on and off, and neither case matches well with experiment. Due to the high temperatures involved, a thermal wave should be expected such that the Spitzer-Härm conductivity on case is more likely. A simulation run with an initial temperature of ~ 4 keV might match better with experiment.

Keywords: Blast wave; Laser; Plasma; Simulation

1. INTRODUCTION

In recent years, there has been considerable interest in conducting laser-plasma experiments of relevance to astrophysical research. Results from these experiments can be used to study fundamental physics, as well as benchmark astrophysical codes. The FLASH code is one such astrophysics code, produced at the University of Chicago under the accelerated strategic computing initiative (ASCI), which is being used to study laser-produced astrophysics experiments, as in Calder *et al*. (2002). Blast waves are just one type of laser-plasma experiment of astrophysical interest, which was conducted at a variety of laboratories and simulated with a variety of numerical codes, including Grun *et al*. (2003), Zhang *et al*. (2003), and Peng *et al*. (2003), among many others. Similarly, a blast wave was produced at the Institute of Laser Engineering (ILE) of Osaka University using a high-power laser to irradiate a planar plastic target in a background nitrogen gas. In the present study, the FLASH code will be used in an attempt to simulate this experiment. One problem is ascertaining the initial conditions to input into FLASH since this code does not model laser-solid interactions, but rather has sophisticated modules to simulate the high-temperature, high-speed flow generated by the laser source. Thus, a simplified model for intense laser irradiation of planar targets will be used to estimate initial conditions. No attempt will be made to improve or add physics modules to FLASH. This study will analyze how well the current version of FLASH can simulate the experimental blast wave.

Address correspondence and reprint requests to: D.R. Farley, EPRI Worldwide, 3412 Hillview Avenue, Palo Alto, California 94304. E-mail: dfarley@epri.com

2. EXPERIMENT

One beam of the ILE GEKKO XII laser system is used to irradiate a plastic planar target. The beam impinged the target at an angle of 20°. The laser had a wavelength 1.053 μm, a pulse length of 1 ps, energy of 7.7 J on target, and the optical f/# was 3.8. The laser spot size on target was about 50 μm diameter. Thus, the on target intensity was approximately 10^{17} W/cm^2 at a power of 8×10^{12} W. The plastic (polystyrene, CH) target had a solid density of 1.06 g/cm^3, a thickness of 6 μm, and an average atomic weight of $Z = 3.5$. The vacuum chamber containing the CH target was maintained at a pressure of 5 Torr ambient nitrogen.

One of GEKKO's other laser beams (4ω, $\lambda = 0.26$ μm, 100 ps) was used to probe the blast wave trajectory. The probed CH target was imaged by a knife-edge to a CCD camera such that the camera is looking edge-on to the target (Schlieren technique). The blast wave was imaged at 16 ns after the laser pulse using with the CCD camera, as shown in Figure 1. The pixel resolution is approximately 12 μm. This

image shows regions of relatively high density, such as immediately behind the blast wave shock front. Note that the laser pulse must pass through the background nitrogen gas to reach the target, which causes a cylindrical blast wave in the nitrogen gas. This can be seen in Figure 1 where the radial shock is intersecting the spherical blast wave.

From Figure 1, the size of the high-density region adjacent to the spherical shock front is about 2.5 mm radius at 16 ns. Also, note the high-density structures within the blast wave. An unavoidable laser pre-pulse 10^{-6} to 10^{-7} less power than the main pulse will interact with the CH target and ambient nitrogen gas for approximately 1 ns before the main pulse arrives. This pre-pulse will initiate plasma near the CH target and may dissociate and ionize the nitrogen gas molecules.

3. THEORY

An analytic solution for a blast wave resulting from an instantaneous energy release from a point source was solved by Sedov (1993). A self-similar solution is obtained for the blast shock wave radius for both cylindrical and spherical waves, as given by Zel'dovich and Raizer (1967) and Landau and Lifshitz (1987)

$$R(t) = \beta(Et^2/\rho_0)^{\alpha} \tag{1}$$

where E is the instantaneous energy deposition, t is time; ρ_0 is the ambient gas density in front of the shock wave. The exponent $\alpha = 1/5$ for spherical waves, and $\alpha = 1/4$ for cylindrical waves. The constant β depends on the polytropic coefficient γ, and is nearly 1.0 for typical gases.

This theory is valid for polytropic gases at times much longer than the laser pulse length (1 ps), and for distances not too distant from the source where the blast wave is still strong (i.e., $\rho_1/\rho_0 \sim (\gamma+1)/(\gamma-1)$ where ρ_1 is the shocked density). Also, this theory assumes only one gas with a point source (or line source for cylindrical waves) releasing energy instantaneously. In the present experiment, the "point source" is actually a disk of CH, and the expanding hot CH plasma acts as a piston to initiate the strong shock into the background nitrogen gas. Thus the theory given by Eq. (1) may not be precisely correct for the present experiment. Indeed, from the FLASH simulations significant amounts of CH are found in the high-density layer near the shock front, not just shocked nitrogen. However, at later times the 50 μm laser spot size is much smaller than the blast wave radius such that the laser spot can be considered a point source and Eq. (1) serves as a useful tool in analyzing the temperature effects of the experiment.

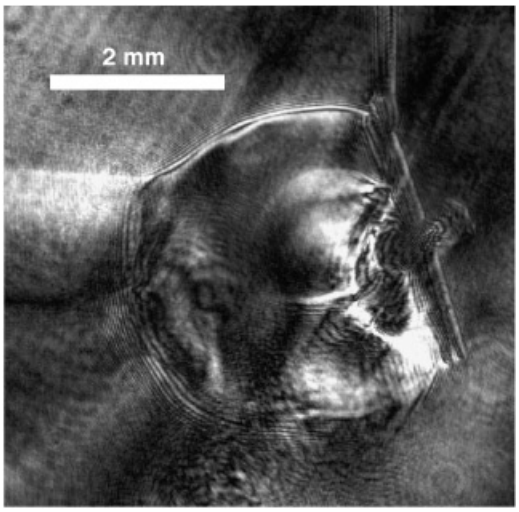

Fig. 1. Blast wave from CH target at 16 ns using laser intensity of 10^{17} W/cm^2 and power of 8×10^{12} W.

At high laser intensities, such as the 10^{17} W/cm^2 involved here, both "cold" and "hot" electrons will be generated. The resulting plasma thus has two species of electrons, each with a Maxwellian distribution. Typical cold temperatures are on the order of 100–1000 eV, while hot electron temperatures will be on the order of 10's of keV. From experimental data at the high laser intensity of the present experiment, the hot electron temperature, T_h, is approximated by Eliezer (2002)

$$T_h(\text{keV}) = 10\left(\frac{I_L\lambda_L^2}{10^{15}\ \text{W}\times\text{cm}^{-2}\times\mu\text{m}^2}\right)^{0.30\pm0.05}. \tag{2}$$

Thus, for the present experiment $T_h \sim 40$ keV. The relative abundance of hot electrons to cold electrons is approximated to be less than 10% at the present laser intensity and angle of laser incidence. Unfortunately, FLASH only allows one temperature, thus neglecting the effect of hot electrons and assuming ion and electron equilibrium.

4. FLASH CODE

FLASH is a modular simulation code capable of handling general compressible flow problems. Adaptive mesh refinement (AMR) is typically used, but a uniform grid can be chosen instead. Supported geometry selections are one-dimensional (1D) spherical, 2D axisymmetric cylindrical, and three-dimensional (3D) Cartesian. The user defines a problem through setting up initial conditions into the mesh domain, including boundary type (i.e., reflecting, outflow, etc.), and then chooses needed physics modules through a simple configuration file. Hydrodynamic modules include the piecewise-parabolic method (PPM) scheme, a Kurganov scheme, and a magnetohydrodynamics (MHD) module. As stated before, the MHD module allows only one temperature. A variety of materials can be used, but to be able to use radiative cooling or ionization and recombination physics modules, only protons (H atoms), electrons, He, C, N, O, Ne, Mg, Si, S, Ar, Ca, Fe, and Ni are available. Other available physics modules include several equations of state (EOS) schemes, nuclear burning, source heating, stirring, gravity, and different options for conductivity and viscosity.

https://doi.org/10.1017/S026303460505069X Published online by Cambridge University Press

FLASH uses the configuration file containing the selected physics modules to automatically select and compile necessary and interdependent lines of code. Note there are no non-physical parameters to alter to force a desired solution (e.g., no flux limiters).

4.1. Radiative cooling

In the hot CH region, the particle number densities are high such that the CH plasma is optically thick. In this region, radiative loss is therefore not significant, but radiative hydrodynamics could be important. Unfortunately, FLASH does not include radiative transfer in the hydrodynamics modules. The hot nitrogen gas region, which is heated by the CH-originated shock wave (with Spitzer-Harm conductivity turned off) or thermal wave (with Spitzer-Harm turned on), is of low enough density as to be optically thin. Radiative loss in this hot nitrogen gas region is therefore possible, but as will be described below is insignificant to the flow development.

The internal energy ε_{int} (erg/g) of the fluid is defined by FLASH as

$$\varepsilon_{\text{int}} = \frac{N_a kT}{\bar{A}(\gamma - 1)}, \tag{3}$$

where N_a is Avogadro's Number, k is Boltzmann's constant, $\bar{A}$ is the average atomic mass for the fluid, and γ is the ideal gas adiabatic index. For diatomic nitrogen, $\bar{A} = 28$ and $\gamma = 1.4$, and temperatures in the hot nitrogen gas region are on the order of 10^7 °K. Thus, the internal energy of the hot nitrogen gas is of the order of 10^{14} erg/g. Radiative cooling $\dot{s}$ (erg/g × s) is given by

$$\dot{s} = \frac{n_e^2 \Lambda(T)}{\rho}, \tag{4}$$

where n_e is the electron density, ρ is the fluid density, and $\Lambda(T)$ is an empirical cooling function available in Raymond *et al*. (1976). For the temperatures of interest, the best case scenario is $\Lambda(T) \sim 10^{-22}$ erg × cm^3/s. Assuming again a best case scenario of full ionization, $n_e = Zn_i = Z\rho N_a/\bar{A}$ where Z is the ionization state (seven for fully ionized N). Mass density in the hot nitrogen region is about 3×10^{-5} g/cm^3, resulting in $\dot{s} \sim 10^{20}$ erg/g × s. A characteristic time of the flow needs to be multiplied by $\dot{s}$ to compare with the internal energy ε_{int}. Another way to look at this is to calculate the time scale in which radiative cooling would be important, such as

$$\frac{\tau_{cool} \cdot \dot{s}}{\varepsilon_{\text{int}}} \cong 0.1 \Rightarrow \tau_{cool} \cong 0.1 \frac{\varepsilon_{\text{int}}}{\dot{s}} \cong 100 \text{ ns} \tag{5}$$

This very large time scale for radiative cooling is well past the experiment time scale, and thus radiative cooling is not important in this experiment.

4.2. Dissociation and ionization

As stated previously, FLASH can calculate electronic ionization and recombination of C, N, and H atoms. However, no consideration is made for diatomic molecules. The question of whether N_2 is fully dissociated is critical to the simulation, both to be able to apply the ionization physics module and to use the correct background pressure for the blast wave. The pressure gradient is the only forcing term in the momentum equation, and the background pressure would double if N_2 is fully dissociated, which therefore would affect the propagation of the blast wave.

Several studies of similar blast wave experiments in a nitrogen background gas were published by MacFarlane *et al*. (1989), Giuliani *et al*. (1989), Laming and Grun (2002), and Laville *et al*. (2004). However, there is no consensus regarding the state of the nitrogen. From MacFarlane *et al*. (1989), the density of diatomic nitrogen was used in the simulation, although they noted that prompt X-rays from the laser-plasma interaction would heat the background gas to 1–2 eV (Ali & McLean, 1985). At these temperatures, nitrogen would be completely dissociated, and partially ionized. However, even if this heat bath were instantly available, it would take time to dissociate. Laming and Grun (2002) assume instant complete dissociation, and Laville *et al*. (2004) account for dissociation in the shock front. Note that none of these simulations were done in full 2D axisymmetric geometry.

The time scale for dissociation can be approximated through the dissociation reaction rate k_f (cm^3/mole × s)

$$\tau_{diss} = \frac{\bar{A}}{\rho k_f}. \tag{6}$$

Reaction rates for high temperature nitrogen can be found in many sources, including Dunn and Kang (1973). The reaction rates for collisions between diatomic molecules ($N_2 + N_2$) and diatomic and atomic nitrogen ($N_2 + N$) are given by

$$k_f = 4.8 \times 10^{17}\, T^{-0.5} \exp(-113000/T) \quad N_2 + N_2 \tag{7a}$$

$$k_f = 4.1 \times 10^{22}\, T^{-1.5} \exp(-113000/T) \quad N_2 + N. \tag{7b}$$

For 2 eV (2.3×10^4°K), $k_f = 2.4 \times 10^{13}$ cm^3/mole × s ($N_2 + N_2$) and $k_f = 8.9 \times 10^{13}$ cm^3/mole × s ($N_2 + N$). For ambient diatomic nitrogen at 5 Torr, the density is 8×10^{-6} g/cm^3 and the dissociation time scale is thus

$$\tau_{diss}\,(2 \text{ eV}) \sim 140 \text{ ns} \quad N_2 + N_2 \tag{8a}$$

$$\tau_{diss}\,(2 \text{ eV}) \sim 40 \text{ ns} \quad N_2 + N. \tag{8b}$$

https://doi.org/10.1017/S026303460505069X Published online by Cambridge University Press

In either case, at temperatures of 2 eV a relatively long time compared to the hydrodynamic time scale is required to dissociate the diatomic nitrogen. Instantaneous dissociation is therefore not justified. This same time scaling can be applied in the hot nitrogen region after shock or thermal wave passage, where the temperature is on the order of 10^{7}°K (~1 keV) and the density is 3×10^{-5} g/cm^3

$$\tau_{diss}\,(1\text{ keV}) \sim 10\text{ ns} \quad N_2 + N_2 \tag{9a}$$

$$\tau_{diss}\,(1\text{ keV}) \sim 500\text{ ns} \quad N_2 + N. \tag{9b}$$

All of these time scales are on the order or larger than the entire experiment. Of course, electron and ion collisions with diatomic molecules have not been considered, which would accelerate dissociation. The point here is that instantaneous dissociation is likely not appropriate, and FLASH cannot account for dissociation effects. Further, since FLASH cannot account for diatomic nitrogen in its ionization physics package, we also cannot use the electronic ionization/recombination module in the present simulations.

Even though ionization cannot be handled by FLASH in this case due to the presence of diatomic nitrogen, an estimate of the typical ionization time scale is useful, as given by Post *et al*. (1977)

$$\tau_{ioniz} \cong 9 \times 10^{5}\,\frac{T(\text{eV})^{3/2}x^2e^{x}}{n_e(1-e^{-x})}, \tag{10}$$

where x is the ionization potential I divided by temperature ($x = I/T$). Note T is in eV in this equation. The first ionization potential for atomic nitrogen is 13 eV, and the electron density in the hot nitrogen region (singly ionized) is $\sim 10^{18}$ cm^{-3} at a temperature of 1 keV, which results in $\tau_{ioniz} \sim 0.4$ ns. The time scale for hydrodynamic flow is similar to this τ_{ioniz} time scale, and thus ionization could be important to flow dynamics. However, MacFarlane *et al*. (1989) noted that ionization affects the fluid flow only at early times very close to the laser spot, and classical collisional hydrodynamics appears to be adequate to model the blast wave evolution after initial time scales.

4.3. Single fluid temperature

FLASH only allows for one temperature, thus always assuming ion and electron temperature equilibrium. In the hot CH region where the densities are high, this may be a valid assumption. However, in the low-density hot nitrogen region, the ion and electron temperatures likely are not in equilibrium. Since this region includes unknown quantities of diatomic nitrogen and various degrees of atomic nitrogen ionization, a time scale calculation for temperature equilibration is difficult. Since a single temperature is only available in FLASH, we cannot comment on the error caused in the simulation due to ion and electron non-equilibrium effects. However, Giuliani *et al*. (1989) did follow both ion and electron temperatures in a similar experiment, and the temperatures appear to be generally similar and in near equilibrium, especially in the blast front region.

5. RESULTS

For the present FLASH simulation, a 2D axisymmetric cylindrical geometry is used with the AMR scheme. FLASH version 2.4 is used. Since magnetic fields are not considered, the MHD module is not used and the hydrodynamic PPM scheme is used instead. The domain size is 3,000 × 3,000 μm in the radial (r) and axial (z) coordinates, with the minimum mesh size being under 0.1 μm in the CH target, which is only 1 μm half-thickness at $z = 0$ (total number of meshes ~ 64000). The $z = 0$ and $r = 0$ boundaries are reflecting, while the $z = 0.3$ cm and $r = 0.3$ cm boundaries are outflows. Having a reflecting boundary at the $z = 0$ location assures a zero velocity at this point. Otherwise, unphysical high velocities occur at $z = 0$. A perfect gas equation of state was assumed for all fluids.

FLASH was run with ionization/recombination and radiative cooling not included, as discussed above. Spitzer-Härm conductivity, given by $\sigma_{SH} = 9.2 \times 10^{-7}T(°\text{K})^{5/2}$ in cgs units, was either turned on or off in the simulations. Spitzer-Härm conductivity was initially turned off to run a faster simulation since the automatically calculated time step of the simulation is inversely proportional to the conductivity. Thus, using σ_{SH} results in a very small time step ($\Delta t \sim T^{-5/2}$) due to the high temperature of the CH, whereas turning Spitzer-Härm off results in a time step several orders of magnitude larger than Spitzer-Härm on case. For example, a typical 2D simulation with Spitzer-Härm off required 2–3 days, but with Spitzer-Härm on required over a month to complete. An Intel Itanium 2 (900 MHz) processor-based Hewlett-Packard workstation was used for these simulations.

Because FLASH is run in 2D, the initial temperature condition of the CH was also assumed to be 2D. Therefore, a Gaussian temperature profile was used for the initial temperature (or equivalently pressure) source, given by

$$T(r) = T_0\,e^{-r^2/2r_0^2}, \tag{11}$$

where $r_0 = 25$ μm corresponding to a laser spot diameter of approximately 50 μm, and $T_0 = 120$ eV. The source temperature of 120 eV was decided from 1D simulation using the Osaka University ILESTA code, which includes laser absorption, ionization and recombination, and relevant EOS physics. Because only basic hydrodynamics, with Spitzer-Härm turned on or off, is used in the present 2D FLASH simulations, the effect of higher or lower T_0 would only change the length scales of the flow, resulting in similar flow morphologies.

According to Ditmire *et al*. (1996), at the high laser power and intensity of the present experiment, a very high speed radiative heat wave will propagate into the plastic upon laser illumination. The time scale for propagating through the

https://doi.org/10.1017/S026303460505069X Published online by Cambridge University Press

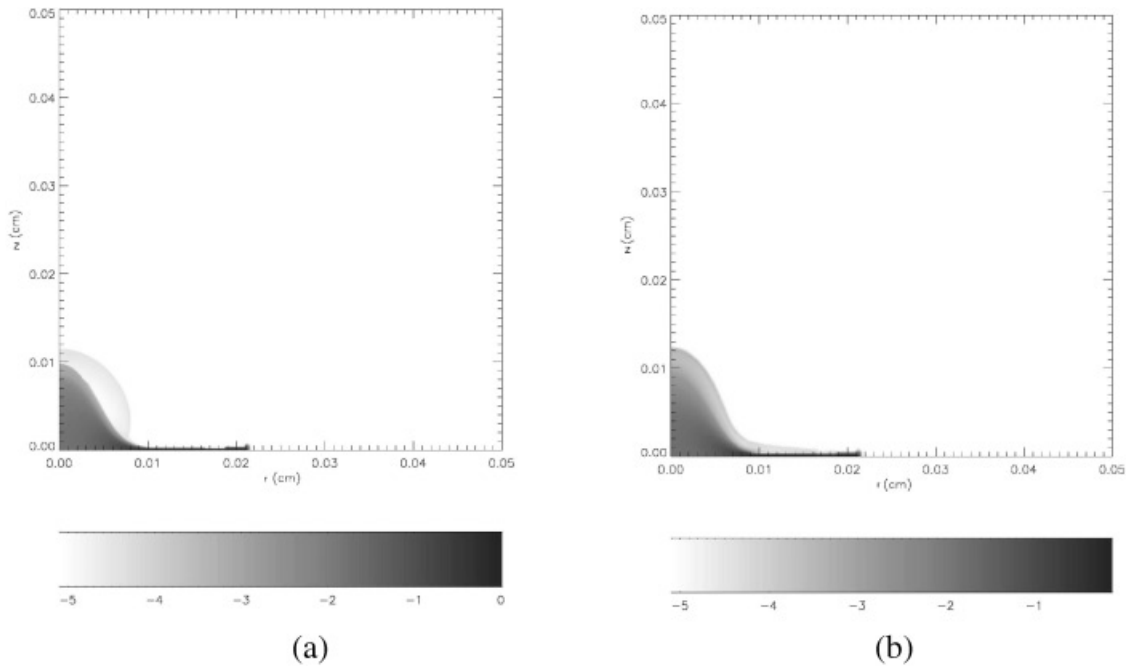

Fig. 2. Density plots (log g/cm^3) at 500 ps for (**a**) Spitzer-Härm OFF and (**b**) Spitzer-Härm ON.

entire 6 μm thickness of the plastic target is estimated to be ∼1 ps. Thus, it is assumed the plastic target is instantly heated to the initial temperature profile given by Eq. (11). Also, the entire slab of CH will not be ablated and accelerated into the nitrogen background, but rather a small part of the CH disk will move into the background gas at a characteristic speed of $\sim 2 \times 10^7$ cm/s. From 1D FLASH simulation, an ablated CH thickness of 1 μm (or less) should be sufficient to initiate a blast wave relevant to the Figure 1 results.

Shown in Figures 2 and 3 are 2D snapshots of density and temperature for Spitzer-Härm conductivity on and off at an

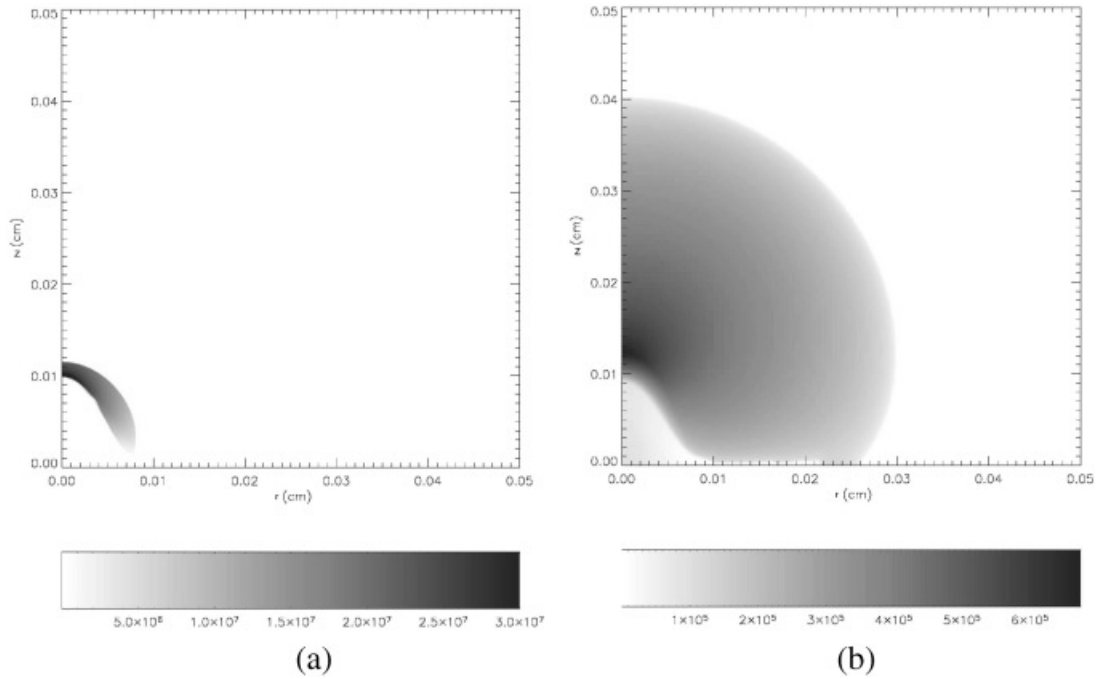

Fig. 3. Temperature plots (°K) at 500 ps for (**a**) Spitzer-Härm OFF and (**b**) Spitzer-Härm ON.

https://doi.org/10.1017/S026303460505069X Published online by Cambridge University Press

early time of 500 ps after laser illumination. As can be seen from Figure 2, the density profiles are quite similar, but the temperature profiles of Figure 3 are very different due to the rapid propagation of a thermal wave resulting from Spitzer-Härm conductivity being included. This Spitzer-Härm thermal wave results in an isothermal temperature of $\sim 10^5$°K behind the wave. The hot CH must then propagate into this high temperature and high pressure nitrogen background. However, this did not cause significant differences in overall wave front propagation between the Spitzer-Härm on and off cases later in time.

Shown in Figure 4 are similar density and temperature plots at 16 ns only for the Spitzer-Härm off case, which is the same time as the experimental result of Figure 1. Note the strong differences between the Spitzer-Härm off case and experiment at this late time. The simulation with Spitzer-Härm on is not shown since the simulation could not finish even after two months of calculating and repeated increases in the minimum mesh size. However, at a time of 2.5 ns (not shown), the propagation speeds are very similar, and the overall blast wave structure are fairly similar for the Spitzer-Härm on and off cases. Therefore, we assume the Spitzer-Härm on and off results at 16 ns will have similar blast wave propagation distances, although the detailed wave structure may differ.

Note that the 120 eV initial temperatures resulted in blast wave propagation about half the size of the experiment. According to Eq. (1), the extent of the blast wave should scale as $T^{1/5}$. Thus, for the blast wave radius to double in size, the temperature should be increased by a factor of 32, which would correspond to $T_0 \sim 4$ keV. It is possible for ion temperatures to be this high, and as previously stated hot electron temperatures should be about 40 keV. Significant physical interaction is likely between ions and electrons at these very high temperatures, and also a likely strong effect on the nitrogen gas close to the CH target. However, none of these physical effects can be modeled by FLASH, even if assuming completely dissociated and ionized materials.

6. CONCLUSIONS

2D FLASH simulations were run with Spitzer-Härm conductivity on and off in an attempt to simulate a laser-produced blast wave. Dissociation, ionization, recombination, and radiative cooling were not included. An initial Gaussian temperature profile with $T_0 = 120$ eV and spot radius $r_0 = 25$ μm was used assuming 1 μm thickness of the CH disk is ablated into the background nitrogen gas. Evolution of the blast wave differs slightly between the cases of Spitzer-Härm on and off, and neither case matches well with experiment. Due to the high temperatures involved, a thermal wave should be expected such that the Spitzer-Härm conductivity on case is more likely. However, all interesting physics occurring near the CH target and corresponding interaction with the background diatomic nitrogen gas has not been considered. As most other authors point out, blast wave evolution can probably be simulated using simple collisional hydrodynamics at time scales much larger than the laser pulse time. The problem is how to decide the appropriate initial conditions to start FLASH after such complicated interactions have subsided.

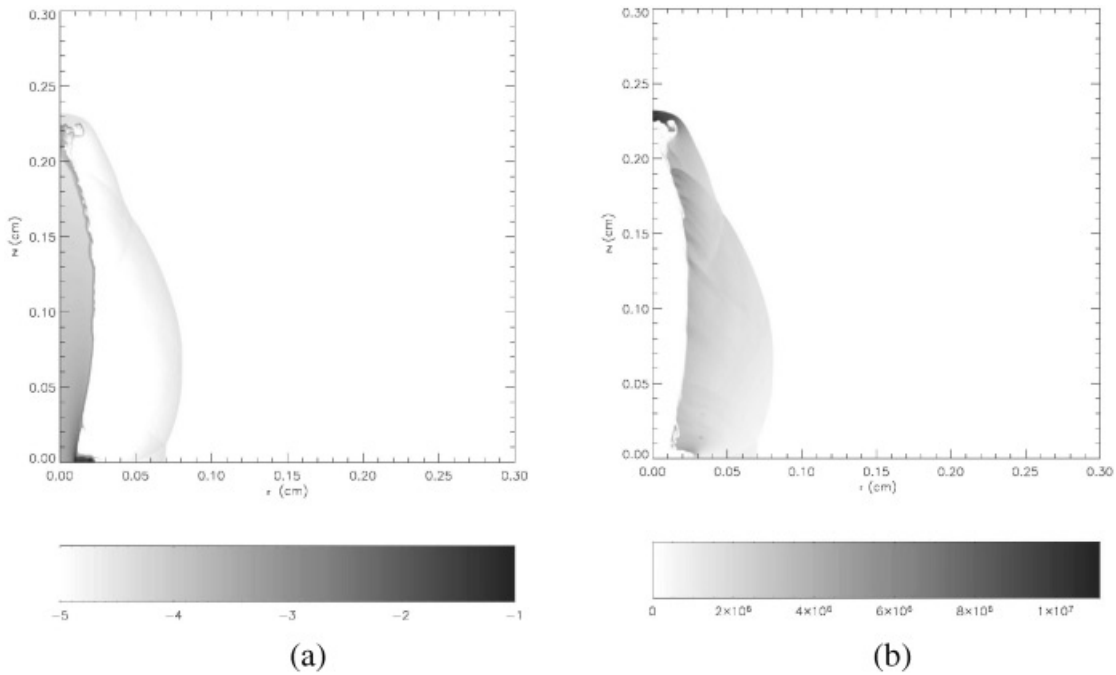

Fig. 4. Plots of Spitzer-Härm off case at 16 ns for (**a**) density (log g/cm^3) and (**b**) temperature (°K).

https://doi.org/10.1017/S026303460505069X Published online by Cambridge University Press

Again, the point of this study was to use FLASH as simply as possible, without changing or adding physics packages, or tuning "knobs" to achieve the desired result. All that was input to FLASH were basic material properties and a simple Gaussian temperature initial source profile. FLASH then automatically proceeds with little interaction required from the user. In fact, the only manipulation done during the simulation runs was to occasionally increase the minimum mesh size to speed up the simulation (note the number of mesh blocks increases as the blast evolves such that the minimum block size can be increased without loss of resolution). It is the authors' view, all of whom are experimentalists, that running a simulation should be done this way. A turn-key simulation code such as FLASH would not be very useful if multiple knobs must be tuned to achieve a desired result, which would produce different results depending on each user. In this sense, we can say the FLASH code stands on its own, with no tuning required, but apparently its included physics packages are inadequate to correctly model the high-temperature laser-produced blast wave of the present experiment. Future work will focus on uncovering which significant physical effects are responsible for the discrepancies between simulation and experiment, and possibly adding magnetic fields to the initial conditions.

ACKNOWLEDGMENTS

The software used in this work was in part developed by the DOE-supported ASCI Alliance Center for Astrophysical Thermonuclear Flashes at the University of Chicago. The authors are also grateful to various researchers at the ASCI FLASH center who offered advice on working with the FLASH code.

REFERENCES

Ali, A.W. & McLean, E.A. (1985). Electron density and temperature in the photoionized background gas (N_2) surrounding a laser-produced plasma. *J. Quant. Spect. Radiat. Trans.* **33**, 381–390.

Calder, A.C., Fryxell, B., Plewa, T., Rosner, R., Dursi, L.J., Weirs, V.G., Dupont, T., Robey, H.F., Kane, J.O., Remington, B.A., Drake, R.P., Dimonte, G., Zingale, M., Timmes, F.X., Olson, K., Ricker, P., MacNeice, P. & Tufo, H.M. (2002). On validating an astrophysical simulation code. *Astrophys. J. Supp.* **143**, 201–230.

Ditmire, T., Gumbrell, E.T., Smith, R.A., Mountford, L. & Hutchinson, M.H.R. (1996). Supersonic ionization wave driven by radiation transport in a short-pulse laser-produced plasma. *Phys. Rev. Lett.* **77**, 498–501.

Dunn, M.G. & Kang, S.W. (1973). Theoretical and experimental studies of reentry plasmas. Contractor Report No. CR-2232. NASA.

Edwards, M.J., MacKinnon, A.J., Zweiback, J., Shigemori, K., Ryutov, D., Rubenchik, A.M., Keilty, K.A., Liang, E., Remington, B.A. & Ditmire, T. (2001). Investigation of ultrafast laser-driven radiative blast waves. *Phys. Rev. Lett.* **87**, 085004.

Eliezer, S. (2002). Thermal conduction and heat waves. In *The Interaction of High-Power Lasers with Plasmas*, p. 202. Bristol: Institute of Physics Publishing.

Giuliani, J.L., Jr., Mulbrandon, M. & Hyman, E. (1989). Numerical simulation of laser-target interaction and blast wave formation. *Phys. Fluids B* **1**, 1463–1476.

Grun, J., Laming, M., Manka, C., Donnelly, D.W., Covington, B.C., Fischer, R.P., Velikovich, A. & Khokhlov, A. (2003). Laser-plasma simulations of astrophysical phenomena and novel applications to semiconductor annealing. *Laser Part. Beams* **21**, 529–534.

Laming, J.M. & Grun, J. (2002). Dynamical overstability of radiative blast waves: The atomic physics of shock stability. *PRL* **89**, 125002.

Landau, L.D. & Lifshitz, E.M. (1987). A strong explosion. In *Fluid Mechanics* (Sykes, J.B. & Reid, W.H., Eds.), 2nd Edition, pp. 403–406. New York: Pergamon Press.

Laville, S., Vidal, F., Johnston, T.W., Chaker, M. & Le Drogoff, B. (2004). Modeling the time evolution of laser-induced plasmas for various pulse durations and fluences. *Phys. Plasmas* **11**, 2182–2190.

MacFarlane, J.J., Moses, G.A. & Peterson, R.R. (1989). Energy deposition and shock wave evolution from laser-generated plasma. *Phys. Fluids B* **1**, 635–643.

Peng, G., Zabusky, N.J. & Zhang, S. (2003). Jet and vortex flows in a shock/hemispherical-bubble-on-wall configuration. *Laser Part. Beams* **21**, 449–453.

Post, D.E., Jensen, R.V., Tarter, C.B., Grasberger, W.H. & Lokke, W.A. (1977). *Atomic Data Nuclear Data Tables* **20**, 397–439.

Raymond, J.C., Cox, D.P. & Smith, B.W. (1976). Radiative cooling of a low-density plasma. *Astrophys. J.* **204**, 290–292.

Sedov, L.I. (1993). Spherical detonation. In *Similarity and Dimensional Methods in Mechanics* (Volkovets, A.G., Ed.), 10th Edition, pp. 240–310. Boca Raton, FL: CRC Press.

Zhang, S., Zabusky, N.J. & Nishihara, K. (2003). Vortex structures and turbulence emerging in a supernova 1987a configuration: interaction of "complex" blast waves and cylindrical/spherical bubbles. *Laser Part. Beams* **21**, 471–477.

Zel'dovich, Y.B. & Raizer, Y.P. (1967). Strong explosion in a homogeneous atmosphere. In *Physics of Shock Waves and High-Temperature Hydrodynamic Phenomena* (Hayes, W.D. & Probstein, R.F., Eds.), pp. 93–101. New York: Academic Press.